

# Direction Symmetry of Wave Field Modulation by Tidal Current

Ina Teutsch <sup>1,2,\*</sup> Saulo Mendes <sup>3,4,5,†</sup> and Jérôme Kasparian <sup>3,4,‡</sup>

<sup>1</sup>*Helmholtz-Zentrum Hereon, Coastal Climate and Regional Sea Level Changes,  
Max-Planck-Straße 1, 21502 Geesthacht, Germany*

<sup>2</sup>*Federal Waterways Engineering and Research Institute (BAW), Hamburg, 22559, Germany*

<sup>3</sup>*Group of Applied Physics, University of Geneva,  
Rue de l'École de Médecine 20, 1205 Geneva, Switzerland*

<sup>4</sup>*Institute for Environmental Sciences, University of Geneva,  
Boulevard Carl-Vogt 66, 1205 Geneva, Switzerland*

<sup>5</sup>*University of Michigan–Shanghai Jiao Tong University Joint Institute,  
Shanghai Jiao Tong University, Shanghai 200240, China*

Theoretical studies on the modulation of unidimensional regular waves over a flat bottom due to a current typically assign an asymmetry between the effects of opposing/following streams on the evolution of major sea variables, such as significant wave height. The significant wave height is expected to monotonically increase with opposing streams and to decrease with following streams. To some extent, observations on data sets containing a few thousand of waves or over a continuous series of about a day confirm this prediction. Based on a multi-year dataset, we show that in very broad-banded seas with high directional spread especially at high values of the ratio between tidal stream and group velocity, the asymptotic behavior of sea variables is highly non-trivial and does not follow the theoretical predictions, thus featuring a symmetrical modulation of several sea state variables respective to whether the current opposes or follows the direction of wave motion.

## I. INTRODUCTION

The deterministic study of inhomogeneous waves sprung near the middle of the twentieth century [1, 2]. Advanced mathematical techniques arose in the following decades [3–6], in particular with wave-current interaction being assessed through ray theory [7, 8], linear wave theory [9, 10], radiation stress [11, 12], action balance [13], spectral [14] and perturbative methods [15]. Through these theoretical advances, transformations of wave characteristics were measured and confirmed in major global currents, such as the Agulhas current [16], the Gulf Stream [17, 18] and the Kuroshio [19, 20]. These transformations concern both significant wave height and wave energy, spectral bandwidth and directional spreading. Additionally, the transformations have been corroborated in laboratory experiments [21–25]. The first studies on wave-current systems focused on tides [1, 26], finding that currents either reduce or expand the wavelength, whose change is met with a modulation in the wave height [1]. These properties of the quasi-stationary and/or homogeneous wave-current systems seem to be universal, featuring similar changes in wave height, length, and period in estuaries and rivers [27–29]. On the other hand, Barber [30] was one of the first to address currents as dominantly changing in time and imply that the absolute period of a near-monochromatic swell is modified following the Doppler effect due to currents, but that the wavelength remains unchanged. As pointed out by Tolman [31], simplified quasi-stationary or quasi-homogeneous

theoretical models based on the action balance equations underestimate the effect of tidal currents on wave heights. Furthermore, Tolman [32] and Holthuijsen and Tolman [17] studied the problem with a full non-stationary and non-homogeneous approach, showing non-local aspects of wave-current interactions in the Southern North Sea and Gulf Stream, respectively.

The majority of the mentioned studies limit the wave-current system to waves encountering an opposing current, resulting in a shortening and steepening of waves due to energy focusing. Only a few studies considered the case of waves propagating in the same direction as the current, and their findings were ambiguous. Theoretical considerations suggested that the wavelength should increase when waves propagate in the same direction as a tidal stream [1]. Indeed, MacIver *et al.* [24] reported from an experimental study that in following currents waves become longer, while at the same time their height is reduced. They concluded that in waves with a following current, wave energy is decreased due to the strain rate of the current speed. Swan *et al.* [23], however, found in an experimental study, supported by a numerical model, that the crest-trough unevenness of waves propagating in a following current increases towards higher and sharper wave crests. This unevenness should increase the probability of extreme waves [33–39].

Observational studies to date are mostly focused on deterministic investigations for specific events or short-term time series analysis [40–44], even those with larger data sets [45–48]. Here, we investigate the behavior of the modulation due to the wave-current interaction of long-term series from a statistical point of view, namely of average wave properties. We characterize the symmetry in the evolution of fundamental wave properties in response to opposing and following currents in the lim-

\* [ina.teutsch@baw.de](mailto:ina.teutsch@baw.de)

† [saulo.dasilvamendes@unige.ch](mailto:saulo.dasilvamendes@unige.ch)

‡ [jerome.kasparian@unige.ch](mailto:jerome.kasparian@unige.ch)

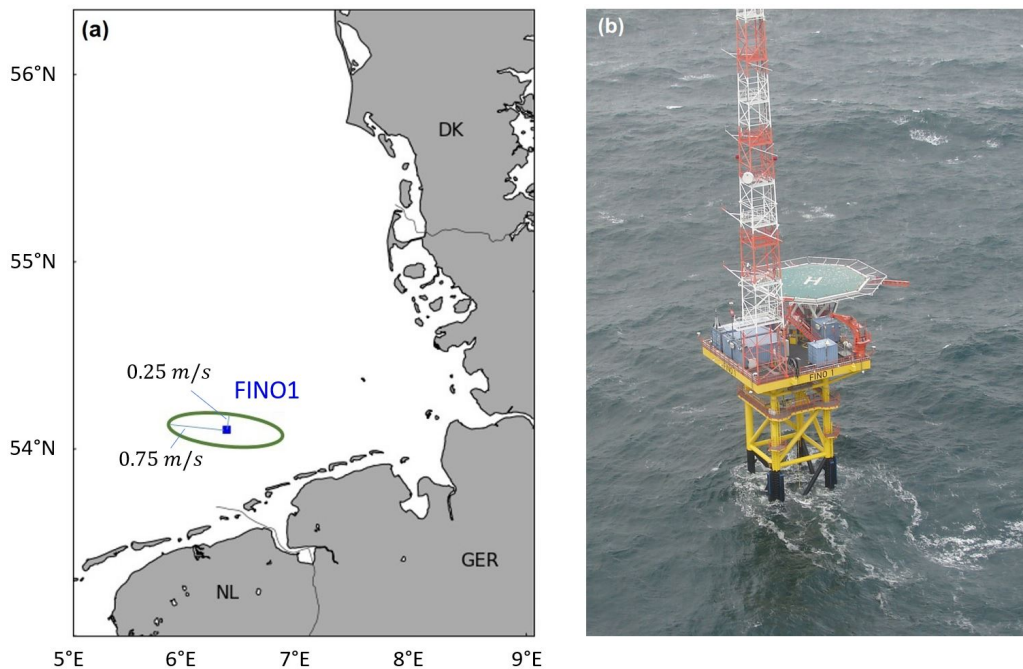


FIG. 1: (a) Location of the research platform FINO1 in the southern North Sea, close to the Dutch and German Frisian islands. The green ellipse indicates the tidal cycle at the site, with semi-major and semi-minor axes of approximately 0.75 m/s and 0.25 m/s, respectively. (b) The research platform FINO1 has been constructed close to the wind farm Alpha Ventus in the North Sea to observe hydrographical and meteorological parameters, among others. ©Forschungs- und Entwicklungszentrum Fachhochschule Kiel GmbH

ited context of currents being co-linear to the direction of wave motion. We show that the following currents can amplify wave fields in deep water in addition to coastal waters [43] and that both the nonlinearity of the sea state and the speed of the tidal stream impact the magnitude and asymmetry of the modulation.

## II. DATA AND METHODS

Wave and current data were recorded between July 2019 and December 2022 at about 200 m distance from the research platform FINO1 in the southern North Sea, which is located at  $54.015^\circ\text{N}$   $6.588^\circ\text{E}$  in a water depth of approximately 30 m (figure 1). The currents at this site result from the tidal cycle, which forms an ellipse with a major axis stretching approximately from west-northwest to east-southeast (figure 1). Waves typically propagated either towards the southeast or towards the east, with peak wave frequencies between 0.11 Hz and 0.14 Hz (figure 2). A more detailed description, of the tidal current in this region, including a tidal chart, can e.g. be found in Reynaud and Dalrymple [49].

Wave elevation data were recorded by a surface-following directional Waverider buoy of type MkIII. The sampling frequency was 1.28 Hz. The resolution of the wave buoy is specified as 0.01 m, with an accuracy of less than 0.5% of the measured surface elevation relative to

Wave parameters	Definition
Peak wavelength $\lambda_p$	Solution to $(\frac{2\pi}{T_p})^2 = \frac{2\pi g}{\lambda_p} \tanh(\frac{2\pi h}{\lambda_p})$
Peak wave number	$k_p = \frac{2\pi}{\lambda_p}$
Relative water depth	$k_p h$
group velocity	$c_g = \frac{1}{2} \sqrt{\frac{g}{k_p} \tanh(k_p h)} \cdot (1 + \frac{2k_p h}{\sinh(2k_p h)})$
Spectral bandwidth	$\nu = \sqrt{\frac{m_0 m_2}{m_1^2} - 1}$
Steepness	$\varepsilon = k_p H_s$

TABLE I: Sea parameter definitions, with gravity  $g$  and spectral moments  $m_n$  assuming small current effects.

the calibrated still water line [51]. The wave buoy delivered surface elevation data in samples of 30 minutes in length, containing 366 waves on average. The samples were quality-controlled according to the procedure described in Teutsch *et al.* [52] and subsequently used to calculate the directional spectra (figure 2a,b) and the sea state parameters in table I for the finite water depth waves without current effects. The current effect on dispersion has ramifications to all other variables, and reads (bold denotes vectors) [11]:

$$\omega = \omega_0 + \mathbf{U} \cdot \mathbf{k} \quad , \quad \omega_0 = g|\mathbf{k}| \tanh |\mathbf{k}|h \quad (1)$$

thus leading to,

$$\omega_0^2 = \omega^2 \left( 1 - \frac{\mathbf{U} \cdot \mathbf{k}}{\omega} \right)^2 = g|\mathbf{k}| \tanh |\mathbf{k}|h \quad (2)$$

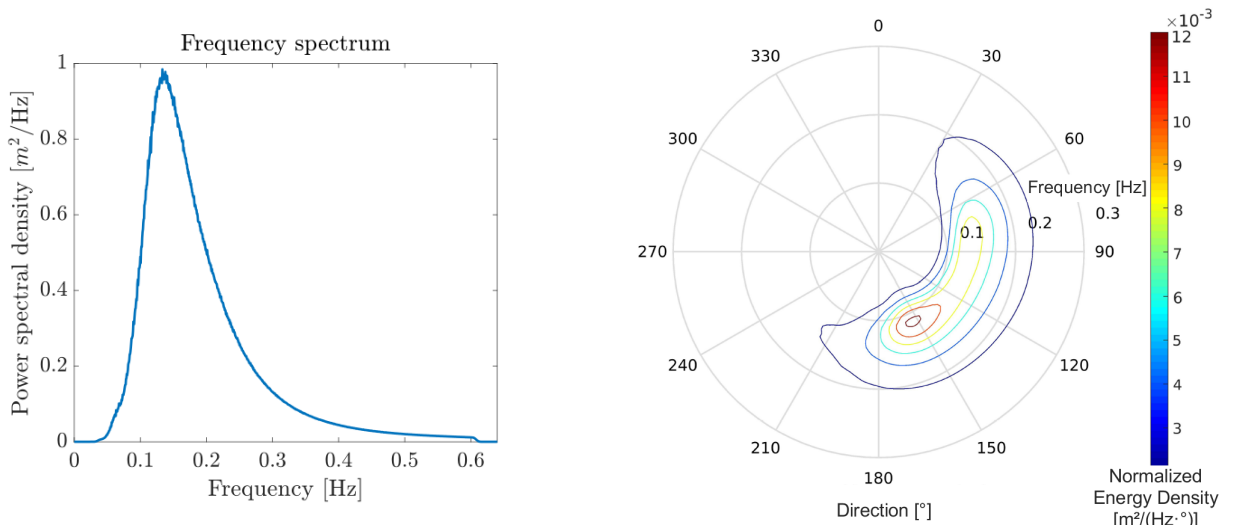


FIG. 2: Mean wave spectra during the period between 2019 and 2022 at the considered site. (a) Unfiltered one-dimensional spectrum. (b) Mean directional wave spectrum, calculated using the DIrectional WAve SPectra Toolbox [DIWASP; 50].

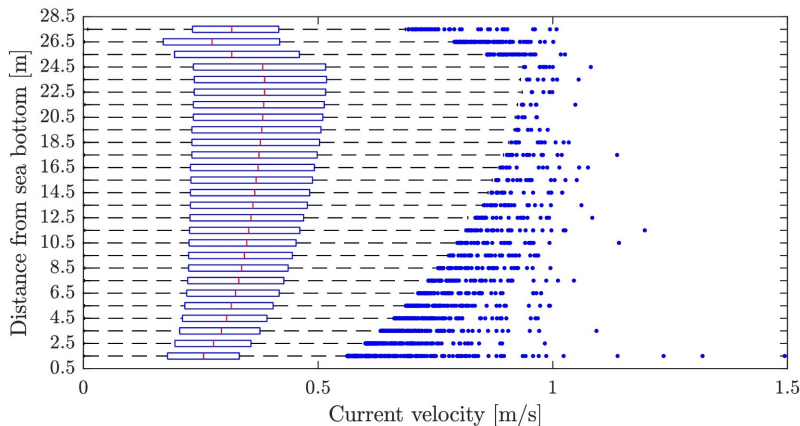


FIG. 3: Box plot of approximately 40,000 measured current speed profiles during the considered time period of 3.5 years. Boxes enclose the two central quartiles with the median in red, while the whiskers encompass from the 25<sup>th</sup> to 75<sup>th</sup> percentiles and the blue markers indicate outliers of the distributions.

As observed in figure 4, most of the data lies in the deep water regime, such that the hyperbolic function has small impact on the dispersion. Moreover, the typical values of the variables measured by their peak parameters show that  $U \sim \pm 0.5\text{m/s}$ , has periods of  $T_p \sim 6\text{s}$  and length  $\lambda_p \sim 75\text{m}$  and therefore the correction due to the current on the dispersion is small  $\mathbf{U} \cdot \mathbf{k}/\omega \sim UT_p/\lambda_p \approx 0.04 \ll 1$ . Therefore, we can compute peak spectral parameters without taking into account the current effect.

Current velocities and directions were recorded by an acoustic Doppler current profiler (ADCP, Nortek), which was deployed at the sea bottom in an approximate water depth of 30 m. The current data made available to us by the Federal Maritime and Hydrographic Agency (BSH) were already quality-controlled using the Storm software provided by the manufacturer [53]. This included correc-

tions for a possible tilt of the instrument and the removal of echo spikes, among others. The ADCP delivered current speeds averaged over a time window of 10 minutes. These current speeds were further time-averaged over the whole duration of each wave elevation sample. Samples with missing wave or current data were excluded from the analysis.

The current speed has a smooth mean vertical profile except at the boundaries (figure 3). Close to the bottom and the surface, wave movements, tidal elevation and sidelobe interference of the ADCP [54] perturb the measurement. Furthermore, the peak frequency of 0.12 Hz (see figure 2a) corresponds to wavelengths of more than 100 m, much larger than the water depth of 30 m. Waves are therefore sensitive to the current in the entire water column, although their sensitivity slightly

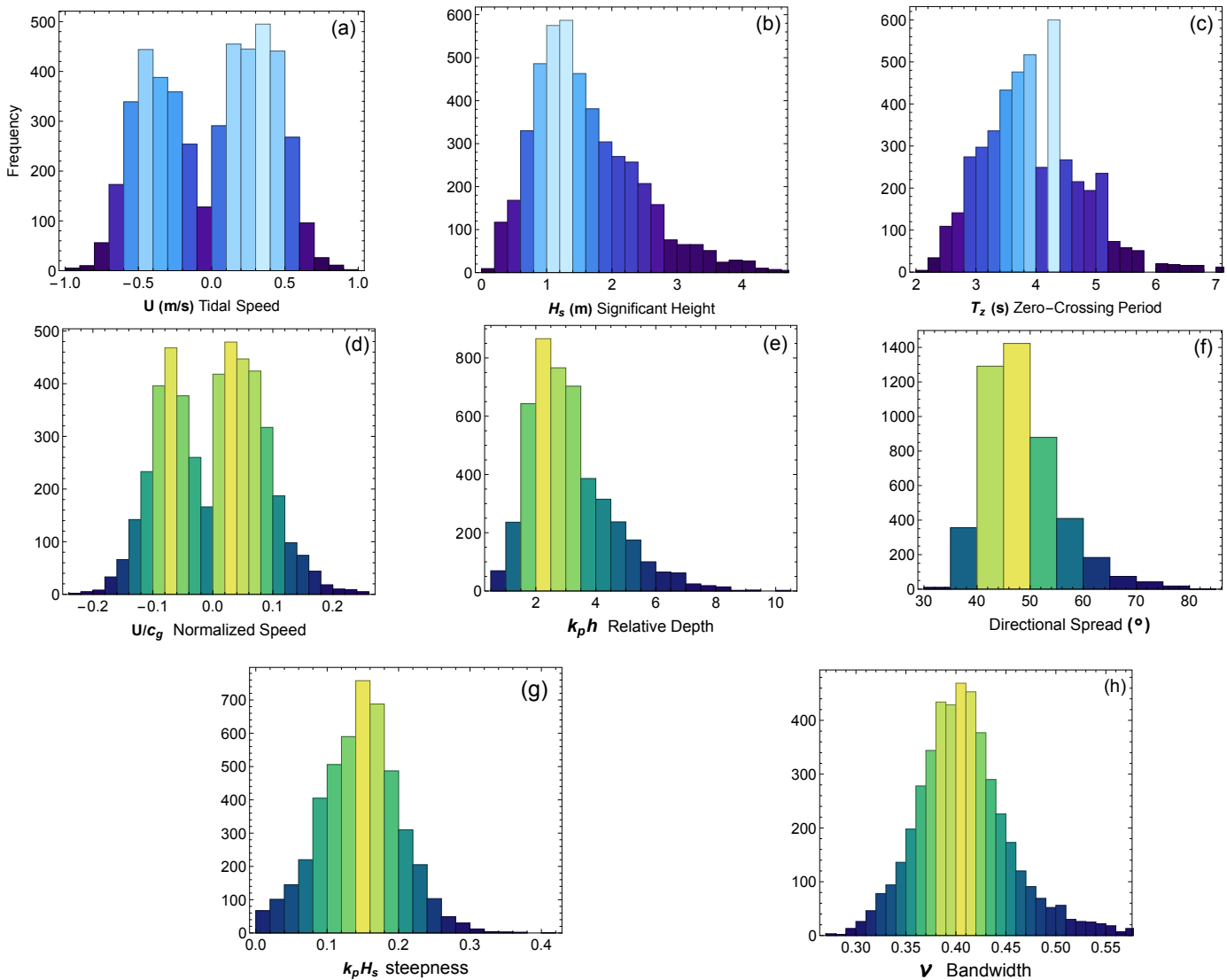


FIG. 4: Histograms of the frequency of 30-minute wave records as a function of the major dimensional variables, as well as normalized current speed. Brighter colors emphasize higher probability density.

decays with the depth. Hence, we considered the current speed approximately 6 m below the water surface (i.e., 24.5 m above the bottom, [figure 3](#)), as representative of the whole column.

Furthermore, current turbulence generated in the water column by the waves [23] via bottom friction [55] may also feedback on the waves themselves. The mixed layer depth, in which turbulence may be generated by surface waves, ranges between 2 m and 6 m in our conditions [56, eq. 7]. Although this feedback likely averages out over the column in our measurements, we verified that neither wave-induced current turbulence, nor our choice of considering the current at 6 m depth influenced the results: repeating the analysis while considering the speed in the middle of the water column (15 m depth) or the (vector) averaged speed between 7.5 m and 22.5 m yielded similar results, as will be discussed in detail in the next section

(see also [figure 6](#)).

Wave direction is defined as the propagation direction of the waves at the peak frequency in the directional wave spectrum,  $\Theta_p$ . The directional spreading of the waves around the peak frequency is calculated as

$$\sigma_{\Theta_p} = \sqrt{2(1 - C_1)}, \quad (3)$$

with  $C_1 = \sqrt{a_1^2 + b_1^2}$ , in which  $a_1$  and  $b_1$  denote the first sine and cosine Fourier coefficients of the directional spectrum, respectively [57]. Note that alternative and equivalent descriptions for the directional spectrum and spreading exist, such as directional spread  $\sigma_\theta = \sqrt{2(1 + s)}$  arriving from a spectral function  $D(\theta) \sim \cos^{2s}(\theta/2)$  [58]. The significant wave height  $H_s$  was computed as the mean of the highest third of waves in each 30-minute sample. To evaluate the effect of current speed  $U$  and current direction on major sea state parameters, we selected two

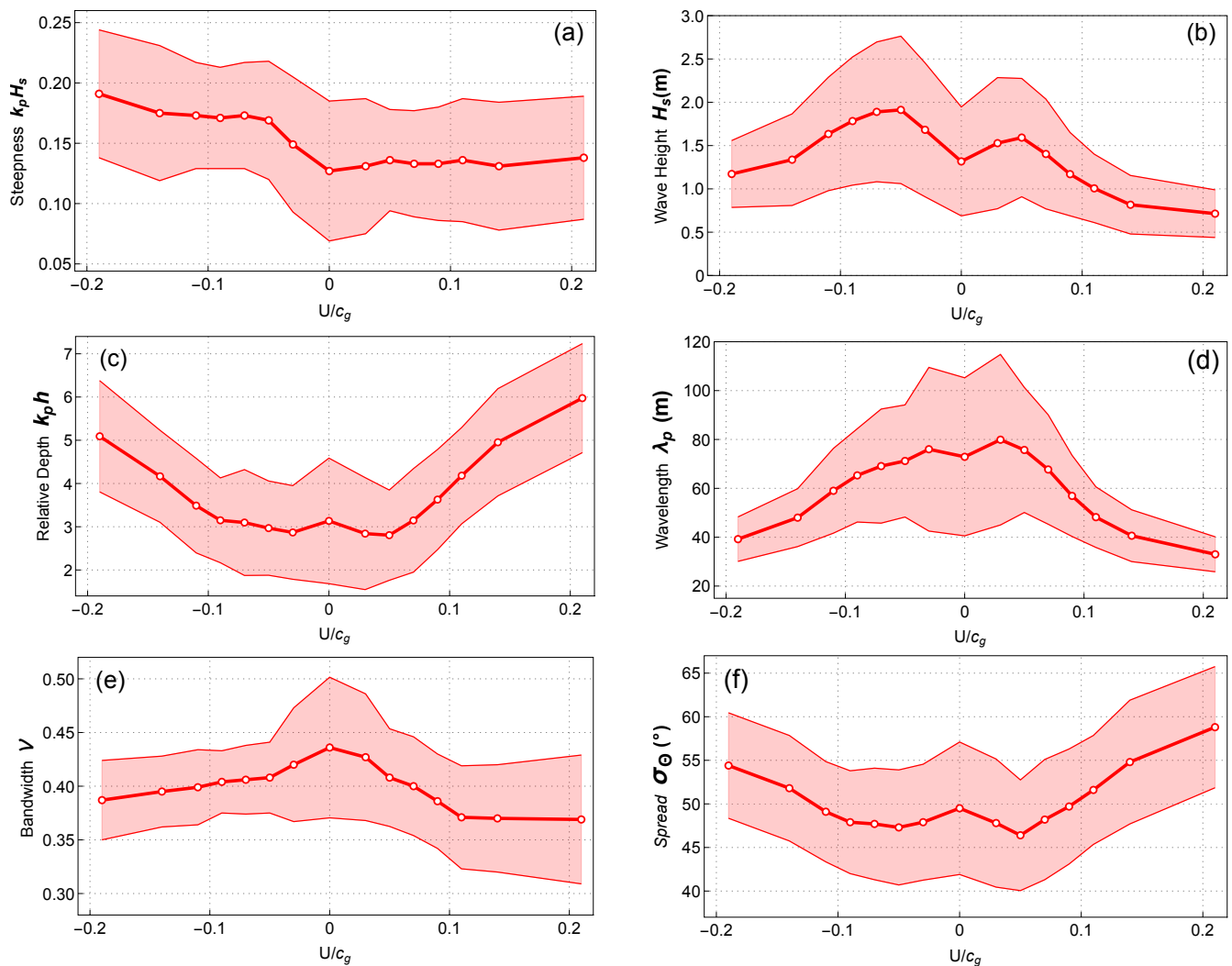


FIG. 5: Average values of the sea state parameters as a function of the relative current speed. Red bands depict plus or minus one standard deviation on the wave data.

sets of samples, for which the angle between peak wave direction and current direction was either  $0 \pm 10^\circ$  (henceforth referred to as "following current") or  $180 \pm 10^\circ$  (henceforth referred to as "opposing current"). Within these ranges, sine values keep below 0.17 and cosine values stay beyond  $\pm 0.98$ , so that the transverse flow is negligible and the axial current is virtually unaffected. References without current, hereafter denoted rest conditions, were defined as samples with  $|U/c_g| < 0.02$ ,  $c_g$  being the group velocity of the peak frequency of the wave spectrum. This threshold is consistent with the residual transverse current at current incidence angles of  $\pm 10^\circ$ .

In total, the quality-controlled data set contained 4686 samples (2156 with opposing current, 2321 with following current, 209 in rest conditions). Values of  $U/c_g$  were binned in intervals of  $\sim 1/50$ , except around zero, where a single bin covers  $|U/c_g| \leq 0.02$ , and for the outermost bins, where data are sparser.

The histograms in figure 4 provide descriptive statistics

of all selected 30 minute samples along the entire data set. Figures 4a,d describe the near-symmetrical character of the tidal speeds, whether in dimensional units or normalized by the peak group velocity. Figures 4b,c provide the wave climate of the region, with mild sea characteristics for both significant wave height and zero-crossing period. Most of the data is in intermediate ( $k_p h = 0.3 - 3.1$ , 47% of the dataset) to deep water ( $k_p h > \pi$ , 50% of the dataset, or even 79% corresponding to  $k_p h \geq 2$ ) (figure 4e). Adding to the complexity of the sea conditions, the spectrum is significantly directionally spread (figure 4f). Furthermore, the spectrum is very broad (Figure 4h). The sea is composed of waves typically of second order in wave steepness ( $0.05 \leq \varepsilon \leq 0.09$ ) [59], albeit smaller fractions of the dataset are also of first and higher orders (figure 4g). To be precise, Stokes expansion of the velocity potential and surface elevation allows us to describe water waves even with fifth-order theory [60] regardless of the numerical value of  $\varepsilon$ . Nonetheless, in the range



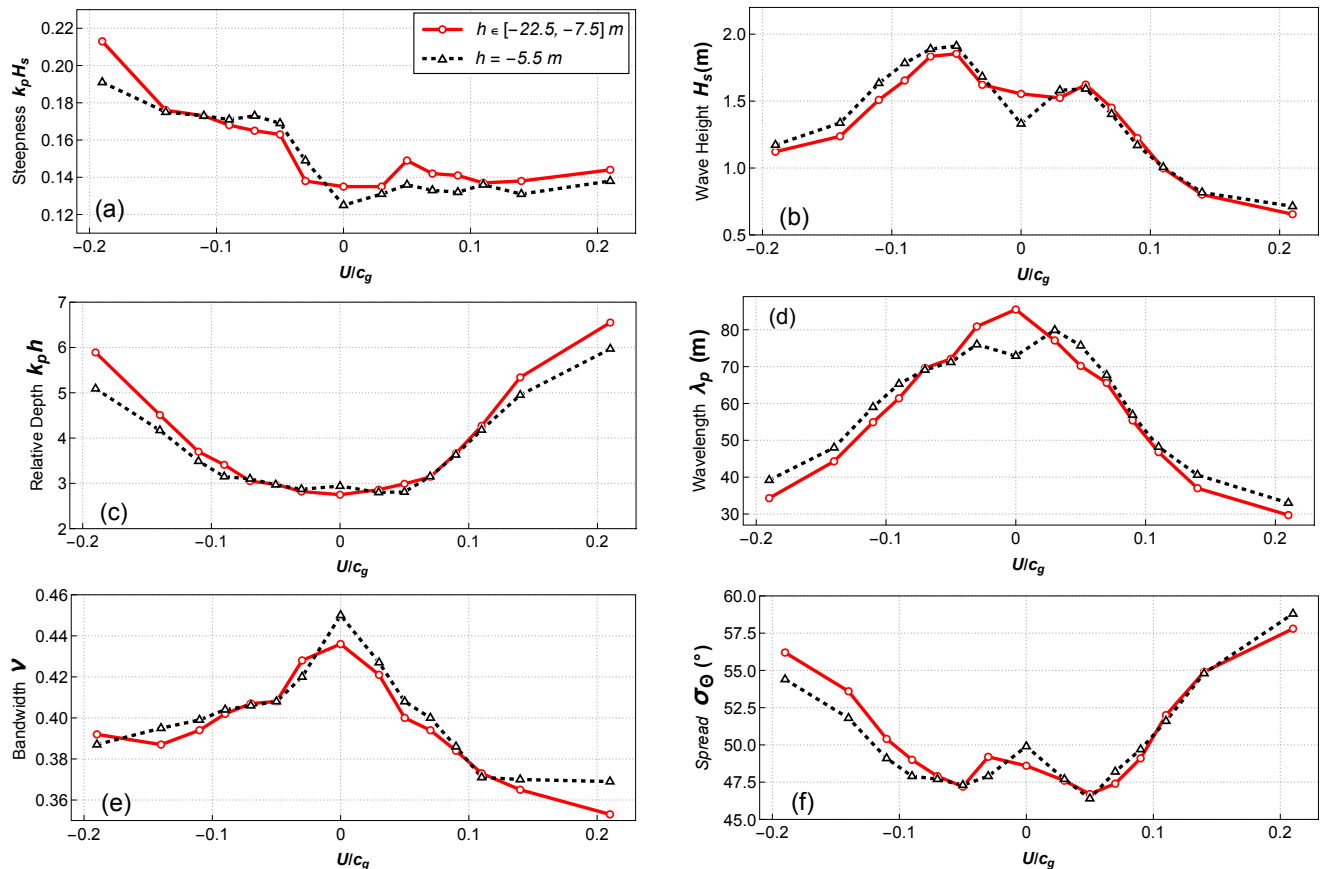


FIG. 6: Sensitivity of results to the depth at which the current speed is measured: Average values of the sea parameters as a function of the relative current speed. The red curves are taken as a function of the normalized speed measured as an average between the 25th and 75th percentile of the water depth ( $-22.5 \text{ m} < h < -7.5 \text{ m}$ ).

$0.05 \leq \varepsilon \leq 0.09$  the second-order theory is sufficient. As discussed in the next section, this strong nonlinearity will be key to the physical behavior of the waves. Typically, consideration of the nonlinear regime of the wave steepness and its effect on wave-tide modulation is overlooked in most studies.

### III. RESULTS

Figure 5 displays the dependence of the main wave parameters on the relative current velocity. Note that there are two ways to normalize the current: either by the current-free group velocity  $\mathbf{c}_g$  or the total group velocity  $\mathbf{c}_h = \mathbf{c}_g + \mathbf{U}$  that is affected by the current. Following Longuet-Higgins and Stewart [11], since we are dealing with data whose collected waves are co-linear to the current we can write the normalized speed as either  $U/c_g = \gamma$  or alternatively  $U/c_h \equiv \gamma/(1 + \gamma)$ . One can verify that the modulations in amplitude and wavenumber described by Longuet-Higgins and Stewart [11] can all be expressed as functions of  $\gamma$  without further algebra to otherwise have functions of  $\gamma/(1 + \gamma)$ . Thus, we proceed to plot normalized velocities in the direction of

motion as  $U/c_g$ . Negative current velocity refers to a current opposing the peak wave direction. Only the mean wave steepness (figure 5a) displays a clear asymmetry between forward and opposing currents. In spite of the wide absolute confidence ranges, the size of the samples is quite large, typically with 100,000 entries per bin. As such, pairwise Welch's  $t$ -tests [61] show a highly significant difference ( $p < 10^{-3}$ ) between bins corresponding to forward and opposing currents of the same speed,  $\pm U/c_g$ , for all pairs of bins.

Other variables display a much more symmetric behavior. The anticipated increase in significant wave height due to an opposing current [1, 10] is observed in our data (figure 5b), but restricted to  $|U/c_g| \leq 0.05$ . Beyond, this trend is inverted and  $H_s$  decreases again. This decrease might be due to either wave blocking [62] or increasing dissipation due to high mean steepness, although it seems to appear earlier than expected by Toffoli *et al.* [63]. The behavior is comparable to the effect of following currents:  $H_s$  increases for mild current speeds, unlike the expected behavior of regular waves [24]. As in the case of an opposing stream, the significant wave height decreases for  $U/c_g > 0.05$ , likely due to wave dissipation.

As expected due to the Doppler effect [10], wavelength

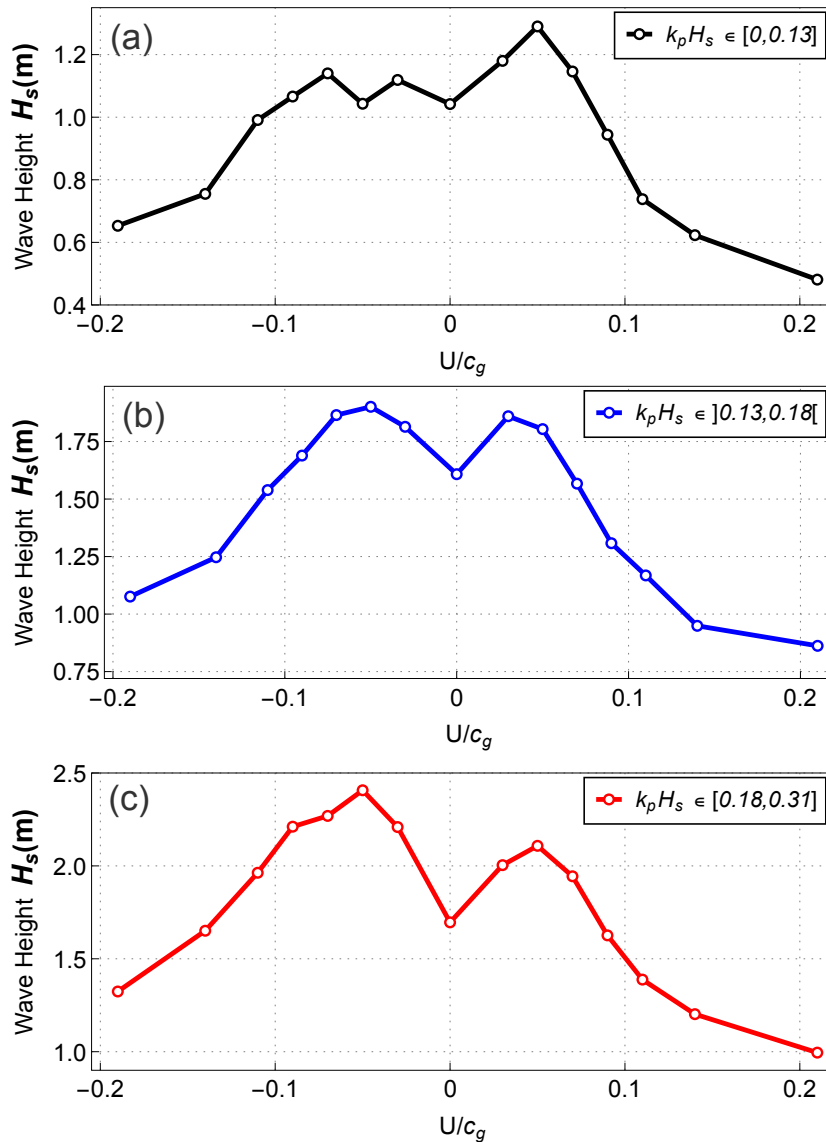


FIG. 7: Average values of the significant wave height as a function of the relative current speed with varying levels of nonlinearity.

is downshifted by an opposing current, and upshifted by a slight following current (figure 5d) for mild current speeds. However, over most of the considered range of following current ( $U/c_g > 0.03$ ), the wavelength shifts back down almost symmetrically to the opposing current. Accordingly, this symmetry also appears (although with an inverted shape) in the relative water depth  $k_p h$  (figure 5c). From the point of view of the classical treatment of waves interacting with uniform currents, this reversal of the Doppler effect is unexpected [10]. For the spectral bandwidth and directional spread, both parameters show symmetrical and bell-shaped responses to the following and opposing currents (figures 5e,f).

From the classical literature [10], we know that the dispersion relation of narrow-banded, unidirectional, and linear waves is affected by the presence of a current: The

dispersion relation  $\omega_0^2 = gk_0$  becomes  $(\omega \pm Uk)^2 = gk_0$ . Bearing in mind that in deep water  $\omega/k = c_p = 2c_g$ , with  $c_p$  denoting the phase speed, one finds the modulation of the wave number to be of the order of,

$$\frac{k}{k_0} \approx \frac{1}{[1 \pm (U/2c_g)]^2} \approx 1 \mp (U/c_g) + 3/4(U/c_g)^2 \quad . \quad (4)$$

When  $|U/c_g| \ll 0.1$ , this modulation is expected to be strongly asymmetrical, however larger values of  $U/c_g = \gamma$  will diminish such asymmetry, as the quadratic term increases and tends to dominate. A less simplistic computation can be performed for non-homogeneous currents, and Longuet-Higgins and Stewart [11] showed that polynomials with order of  $\gamma$  and  $\gamma^2$  will appear. Furthermore, the wave theory for steeper waves leads to a strengthening of the quadratic term [64–66], in addition to shear

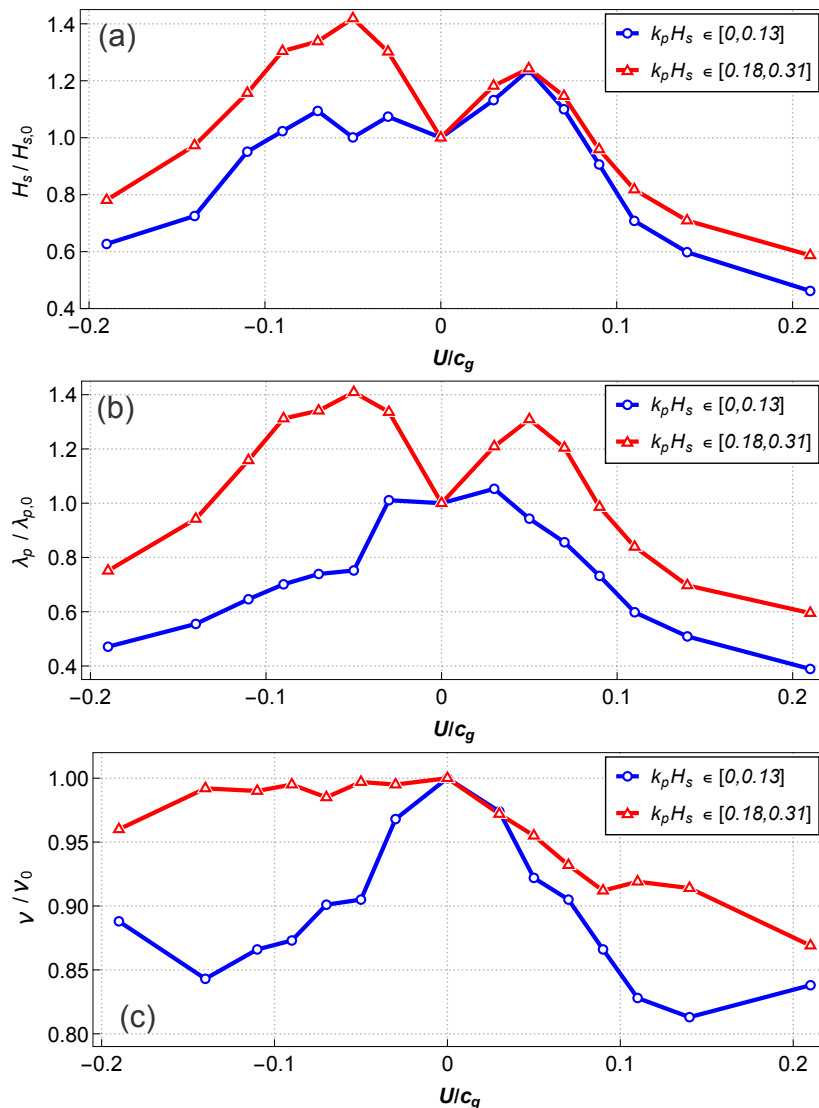


FIG. 8: Relative change in the average values of significant wave height, wavelength, and bandwidth as a function of normalized tidal stream speed over different partitions of the North Sea data.

terms [23, 67]. Besides, from the dynamic point of view, Ho *et al.* [43] showed that the relevant parameter is the phase speed of the current relative to the wave group velocity, so that the interaction between a following current and a comparatively slow wave field in the fixed frame appears to be an interaction between an opposing current and waves in the reference frame of the tide.

To rule out artifacts related to the depth at which the tidal stream speed was considered, we compared the previous analysis to its counterpart performed at the middle point of the column ( $h = -15$  m). These returned very similar results. Note that deeper data typically features 10% more samples, due to the reduced perturbations of the ADCP signal. Averaging the velocity between 7.5 and 22.5 m depth also provided similar results, depicted in figure 6.

The symmetric behavior of the significant wave height

in figure 5b with regard to the direction of the tidal current  $U/c_g$  mixes different sea states covering a wide range of nonlinearity (or, equivalently, the wave steepness  $\varepsilon$ , see figure 4g). Due to higher-order corrections to the dispersion relation [64, 65], different effects of current velocity on wavelength and bandwidth can be expected for different levels of nonlinearity. We partitioned the data into three ranges of wave steepness, in accordance with Lé Méhauté's diagram, considering a similar number of waves in each group.

For a low nonlinearity ( $\varepsilon \leq 0.06$ ), the response of the significant wave height to tidal stream speeds is slightly skewed to the right for  $|U/c_g| < 0.05$ : a following stream boosts the significant wave height more than an opposing one (figure 7a). For waves of higher orders in steepness ( $\varepsilon > 0.08$ ) ranging up to breaking, we observed a higher increase of  $H_s$  for opposing streams, which is the op-



posite of what was observed for linear seas (figure 7c), while intermediate nonlinearities feature an intermediate behavior, with an approximately symmetrical effect of currents on  $H_s$  (figure 7b). These skewnesses are highly significant, the Welch's  $t$ -test between bins with forward and opposing streams of equal speed displaying  $p$  values smaller than  $10^{-3}$ .

In all cases, the significant wave height was damped by currents, whether opposing or following, beyond  $|U/c_g| > 0.05$ . Note that the pattern observed in figure 7a has been observed previously [47, 68]. Thus, apparent contradictions in the literature regarding the primacy of opposing or following tides on the modulation of the significant wave height might be due to the analysis of different ranges of wave steepness.

Figure 8 superposes the statistics for wavelength and bandwidth, along with significant wave height, for low- and high-nonlinearity ranges, normalized with regard to their value in the central bin  $U/c_g = 0$ . Figure 8a shows that the magnitude of the modulation  $H_s/H_{s,0}$  by an opposing current, relative to the no-current case, is higher in nonlinear than in linear seas.

The wavelength modulation  $\lambda_p/\lambda_{p,0}$  is symmetric relative to  $U/c_g$  regardless of the wave steepness (figure 8b). However, the magnitude of this modulation is larger for higher wave steepness. Conversely, the decay of bandwidth with increasing normalized tidal current speed is quite symmetrical for linear seas and asymmetrical for nonlinear seas (figure 8c). In the latter regime, an opposing current hardly affects the bandwidth, while following currents reduce it.

#### IV. CONCLUSION

We assessed symmetries and asymmetries between the effects of opposing and following currents on wave modulation and their dependence on the normalized tidal speed. We showed that following currents will modulate the wave field as strongly, and sometimes even stronger, as the opposing currents. This strong effect of a following current is somewhat unexpected by the classical wave theory, when linear waves are subject to interaction

with uniform currents [43]. Furthermore, we showed that both opposing and following currents narrow the spectrum but increase its directional spread. Moreover, the asymmetry in the modulation of significant wave height and the Doppler shift between following and opposing currents only meet the classical theoretical expectations at very low normalized current speeds ( $|U/c_g| < 0.03$ ). At higher current speeds, the shape of the modulation is quite symmetrical for all wave parameters except wave steepness. Whether the maximum modulation appears on the opposing or the following current side depends on the nonlinearity of the sea state and the speed of the tidal stream compared to the wave group velocity.

Our main findings corroborate and extend the study of Ho *et al.* [43] regarding the modulation of wave fields by a following current, by extending them up to deep water conditions and providing multi-year observational data ensuring robust statistics. However, future work entails reproduction of these findings in the laboratory. By isolating the effects of current speed, bandwidth and directional spread, this could support the elaboration of new theoretical understanding of the modification of the dispersion relation by tidal currents.

#### V. ACKNOWLEDGEMENTS

The measurement data were collected and made freely available by the BSH marine environmental monitoring network (MARNET), the RAVE project ([www.rave-offshore.de](http://www.rave-offshore.de)), the FINO project ([www.fino-offshore.de](http://www.fino-offshore.de)) and cooperation partners of the BSH. The sea state portal was realized by the RAVE project (Research at alpha ventus), which was funded by the Federal Ministry for Economic Affairs and Climate Action on the basis of a resolution of the German Bundestag.

#### VI. DATA AVAILABILITY STATEMENT

The underlying wave buoy and ACDP data are the property of and were made available by then Federal Maritime and Hydrographic Agency, Germany. They can be obtained upon request from these organizations.

- 
- [1] P. J. H. Unna, Waves and tidal streams, *Nature* **149**, 219 (1942).
  - [2] J. Johnson, The refraction of surface waves by currents, *Transactions American Geophysical Union* **28**, 867 (1947).
  - [3] F. Ursell, On kelvin's ship-wave pattern, *Journal of Fluid Mechanics* **8**, 418 (1960).
  - [4] G. B. Whitham, Mass, momentum and energy flux in water waves, *Journal of Fluid Mechanics* **12**, 135 (1962).
  - [5] G. B. Whitham, A general approach to linear and nonlinear dispersive waves using a lagrangian, *Journal of Fluid Mechanics* **22**, 273 (1965).
  - [6] F. P. Bretherton and C. J. R. Garrett, Wavetrains in inhomogeneous moving media, *Proceedings of the Royal Society of London. Series A. Mathematical and Physical Sciences* **302**, 529 (1968).
  - [7] R. S. Arthur, Refraction of shallow water waves: the combined effect of currents and underwater topography, *Transactions American Geophysical Union* **31**, 549 (1950).
  - [8] G. B. Whitham, A note on group velocity, *Journal of Fluid Mechanics* **9**, 347 (1960).

- [9] G. I. Taylor, The action of a surface current used as a breakwater, *Proceedings of the Royal Society of London. Series A. Mathematical and Physical Sciences* **231**, 466 (1955).
- [10] D. H. Peregrine, Interaction of water waves and currents, *Advances in applied mechanics* **16**, 9 (1976).
- [11] M. S. Longuet-Higgins and R. W. Stewart, Changes in the form of short gravity waves on long waves and tidal currents, *Journal of Fluid Mechanics* **8**, 565 (1960).
- [12] M. S. Longuet-Higgins and R. W. Stewart, The changes in amplitude of short gravity waves on steady non-uniform currents, *Journal of Fluid Mechanics* **10**, 529 (1961).
- [13] J. Willebrand, Energy transport in a nonlinear and inhomogeneous random gravity wave field, *Journal of Fluid Mechanics* **70**, 113 (1975).
- [14] N. E. Huang, D. T. Chen, C.-C. Tung, and J. R. Smith, Interactions between steady non-uniform currents and gravity waves with applications for current measurements, *Journal of Physical Oceanography* **2**, 420 (1972).
- [15] W. D. McKee, Waves on a shearing current: a uniformly valid asymptotic solution, in *Mathematical Proceedings of the Cambridge Philosophical Society*, Vol. 75 (1974) pp. 295–301.
- [16] D. E. Irvine and D. G. Tilley, Ocean wave directional spectra and wave-current interaction in the agulhas from the shuttle imaging radar-b synthetic aperture radar, *Journal of Geophysical Research: Oceans* **93**, 15389 (1988).
- [17] L. Holthuijsen and H. Tolman, Effects of the gulf stream on ocean waves, *Journal of Geophysical Research: Oceans* **96**, 12755 (1991).
- [18] D. W. Wang, A. K. Liu, C. Y. Peng, and E. A. Meindl, Wave-current interaction near the gulf stream during the surface wave dynamics experiment, *Journal of Geophysical Research: Oceans* **99**, 5065 (1994).
- [19] P. A. Hwang, Altimeter measurements of wind and wave modulation by the kuroshio in the yellow and east china seas, *Journal of oceanography* **61**, 987 (2005).
- [20] J. Wang, C. Dong, and K. Yu, The influences of the kuroshio on wave characteristics and wave energy distribution in the east china sea, *Deep Sea Research Part I* **158**, 103228 (2020).
- [21] G. P. Thomas, Wave-current interactions: an experimental and numerical study. part 1. linear waves, *Journal of Fluid Mechanics* **110**, 457 (1981).
- [22] G. P. Thomas, Wave-current interactions: an experimental and numerical study. part 2. nonlinear waves, *Journal of Fluid Mechanics* **216**, 505 (1990).
- [23] C. Swan, I. P. Cummins, and R. L. James, An experimental study of two-dimensional surface water waves propagating on depth-varying currents. part 1. regular waves, *Journal of Fluid Mechanics* **428**, 273 (2001).
- [24] R. MacIver, R. Simons, and G. Thomas, Gravity waves interacting with a narrow jet-like current, *Journal of Geophysical Research: Oceans* **111** (2006).
- [25] Y. Ma, G. Dong, M. Perlin, X. Ma, G. Wang, and J. Xu, Laboratory observations of wave evolution, modulation and blocking due to spatially varying opposing currents, *Journal of fluid mechanics* **661**, 108 (2010).
- [26] H. U. Sverdrup, On wave heights in straits and sounds where incoming waves meet a strong, tidal current, *Scripps Inst. Ocean. Wave Report* , 4 (1944).
- [27] F. I. González, A case study of wave-current-bathymetry interactions at the columbia river entrance, *Journal of physical oceanography* **14**, 1065 (1984).
- [28] L. H. Holthuijsen, N. Booij, and T. H. C. Herbers, A prediction model for stationary, short-crested waves in shallow water with ambient currents, *Coastal engineering* **13**, 23 (1989).
- [29] S. Zippel and J. Thomson, Surface wave breaking over sheared currents: Observations from the mouth of the columbia river, *Journal of Geophysical Research: Oceans* **122**, 3311 (2017).
- [30] N. F. Barber, The behaviour of waves on tidal streams, *Proceedings of the Royal Society of London. Series A. Mathematical and Physical Sciences* **198**, 81 (1949).
- [31] H. L. Tolman, The influence of unsteady depths and currents of tides on wind-wave propagation in shelf seas, *Journal of Physical Oceanography* **20**, 1166 (1990).
- [32] H. L. Tolman, Effects of tides and storm surges on north sea wind waves, *Journal of physical oceanography* **21**, 766 (1991).
- [33] T. Marthinsen, On the statistics of irregular second-order waves, Report No. RMS-11 (1992).
- [34] N. Mori and N. Kobayashi, Nonlinear distribution of nearshore free surface and velocity, in *Coastal Engineering 1998* (1998) pp. 189–202.
- [35] N. Mori and T. Yasuda, A weakly non-gaussian model of wave height distribution random wave train, *Ocean Eng.* **29**, 1219–1231 (2002).
- [36] M. A. Tayfun and M. A. Alkhalidi, Distribution of sea-surface elevations in intermediate and shallow water depths, *Coastal Eng.* **157** (2020).
- [37] S. M. S. Mendes, On the statistics of oceanic rogue waves in finite depth: Exceeding probabilities, physical constraints and extreme value theory, UNC Chapel Hill PhD Thesis. (2020).
- [38] S. Mendes, A. Scotti, M. Brunetti, and J. Kasparian, Non-homogeneous model of rogue wave probability evolution over a shoal, *J. Fluid Mech.* **939**, A25 (2022).
- [39] S. Mendes and A. Scotti, The rayleigh-haring-tayfun distribution of wave heights in deep water, *Applied Ocean Research* **113**, 102739 (2021).
- [40] N. Guillou, Modelling effects of tidal currents on waves at a tidal stream energy site, *Renewable Energy* **114**, 180 (2017).
- [41] M. J. Lewis, T. Palmer, R. Hashemi, P. Robins, A. Saulter, J. Brown, H. Lewis, and S. Neill, Wave-tide interaction modulates nearshore wave height, *Ocean Dynamics* **69**, 367 (2019).
- [42] M. A. Barnes and C. Rautenbach, Toward operational wave-current interactions over the agulhas current system, *Journal of Geophysical Research: Oceans* **125**, e2020JC016321 (2020).
- [43] A. Ho, S. Merrifield, and N. Pizzo, Wave-tide interaction for a strongly modulated wave field, *Journal of Physical Oceanography* **53**, 915 (2023).
- [44] L. Jia, R. Wu, F. Shi, B. Han, and Q. Yang, A numerical study of multiscale current effects on waves in the northern south china sea, *Ocean Modelling* , 102342 (2024).
- [45] F. Ardhuin, L. Marié, N. Rasclé, P. Forget, and A. Roland, Observation and estimation of lagrangian, stokes, and eulerian currents induced by wind and waves at the sea surface, *Journal of physical oceanography* **39**, 2820 (2009).

- [46] F. Ardhuin, A. Roland, F. Dumas, A.-C. Bennis, A. Sentchev, P. Forget, J. Wolf, F. Girard, P. Osuna, and M. Benoit, Numerical wave modeling in conditions with strong currents: Dissipation, refraction, and relative wind, *Journal of Physical Oceanography* **42**, 2101 (2012).
- [47] J. Gemmrich and C. Garrett, The signature of inertial and tidal currents in offshore wave records, *Journal of physical oceanography* **42**, 1051 (2012).
- [48] T. Halsne, A. Benetazzo, F. Barbariol, K. H. Christensen, A. Carrasco, and Ø. Breivik, Wave modulation in a strong tidal current and its impact on extreme waves, *Journal of Physical Oceanography* **54**, 131 (2024).
- [49] J.-Y. Reynaud and R. W. Dalrymple, Shallow-marine tidal deposits, in *Principles of Tidal Sedimentology*, edited by R. A. Davis Jr. and R. W. Dalrymple (Springer Netherlands, Dordrecht, 2012) pp. 335–369.
- [50] D. Johnson, Diwasp, a directional wave spectra toolbox for matlab®: User manual, Centre for Water Research, University of Western Australia. (2002).
- [51] Datawell, [Datawell directional waverider mkiii](#) (2023), accessed on September 04, 2023.
- [52] I. Teutsch, R. Weisse, J. Moeller, and O. Krueger, A statistical analysis of rogue waves in the southern north sea, *Natural Hazards and Earth System Sciences* **20**, 2665 (2020).
- [53] Nortek, Storm postprocessing software, [NortekSoftware](#) (2022), version 1.17.11.
- [54] Nortek, The comprehensive manual for adcps, [Nortek](#) (2022).
- [55] J. Wolf and D. Prandle, Some observations of wave-current interaction, *Coastal Engineering* **37**, 471 (1999).
- [56] A. V. Babanin, On a wave-induced turbulence and a wave-mixed upper ocean layer, *Geophysical Research Letters* **33**, [10.1029/2006gl027308](#) (2006).
- [57] A. J. Kuik, G. P. Van Vledder, and L. H. Holthuijsen, A method for the routine analysis of pitch-and-roll buoy wave data, *Journal of physical oceanography* **18**, 1020 (1988).
- [58] H. Mitsuyasu, F. Tasai, T. Suhara, S. Mizuno, M. Ohkusu, T. Honda, and K. Rikiishi, Observations of the directional spectrum of ocean waves using a cloverleaf buoy, *Journal of Physical Oceanography* **5**, 750 (1975).
- [59] B. Lé Méhauté, *An introduction to hydrodynamics and water waves*, Springer (1976).
- [60] J. Fenton, A fifth-order stokes theory for steady waves, *Journal of Waterway, Port, Coastal and Ocean Engineering* **111**, 216 (1985).
- [61] B. L. Welch, The generalization of ‘student’s’ problem when several different population variances are involved, *Biometrika* **34**, 28 (1947).
- [62] A. Chawla and J. T. Kirby, Monochromatic and random wave breaking at blocking points, *Journal of Geophysical Research: Oceans* **107**, 4 (2002).
- [63] A. Toffoli, T. Waseda, H. Houtani, T. Kinoshita, K. Collins, D. Proment, and M. Onorato, Excitation of rogue waves in a variable medium: An experimental study on the interaction of water waves and currents, *Physical Review E* **87**, 051201 (2013).
- [64] I. Brevik, Remarks on set-down for wave groups and wave-current systems, *Coastal Engineering* **2**, 313 (1978).
- [65] J. H. Pihl, H. Bredmose, and J. Larsen, Shoaling of sixth-order stokes waves on a current, *Ocean engineering* **28**, 667 (2001).
- [66] I. G. Jonsson, Energy flux and wave action in gravity waves propagating on a current, *Journal of Hydraulic Research* **16**, 223 (1978).
- [67] C. Swan and R. James, A simple analytical model for surface water waves on a depth-varying current, *Applied Ocean Research* **22**, 331 (2000).
- [68] C. E. Vincent, The interaction of wind-generated sea waves with tidal currents, *Journal of Physical Oceanography* **9**, 748 (1979).